Development of a Tomography Camera System with a Doublet Lens Unit for Supersonic Collisional Merging Formation of FRC*)

Keisuke HIRAMA, Reiji HAYATA, Taichi SEKI, Daichi KOBAYASHI, Tsutomu TAKAHASHI and Tomohiko ASAI

Nihon University, Tokyo 101-8308 Japan

(Received 9 January 2023 / Accepted 6 March 2023)

Collisional merging experiments of field-reversed configurations (FRCs) have been conducted in the FRC Amplification via Translation-Collisional Merging device at Nihon University. Self-organized FRCs have been observed after the dynamic process with destructive disturbance of the collision/merging of plasmoids at super-Alfvénic speeds. A compact and component-based tomography camera (T-cam) has been developed to obtain the internal structure of plasmoids during and after the collisional merging process using a computed tomography technique. The plasmoids radially expand by a factor of 2 within a few microseconds in the collision and merging phases. Because the viewing angle of the T-cam was limited by the inner diameter of the observation port, the field of view was insufficient for the accurate reconstruction of the internal structure. In this study, the incident optical component of the T-cam is improved to provide a sufficient viewing angle to observe the whole process of collision and merging of plasmoids. The newly-built component, comprising a doublet lens with two plano-convex cylindrical lenses at different focal lengths, expands the viewing angle from 60° - 100°. Simulation results with dummy data indicate that the internal structure of plasmoids during the dynamic process can be reconstructed with the developed system.

Keywords: field-reversed configuration, collisional merging, computed tomography

DOI: 10.1585/pfr.18.2401028

1. Introduction

Field-reversed configuration (FRC) plasma, a type of magnetic confinement plasma, ideally possesses a purely poloidal magnetic flux and maintains its magnetic configuration using toroidal plasma current [1].

At Nihon University, collisional merging experiments of FRC have been conducted on the FRC Amplification via Translation-Collisional Merging (FAT-CM) device [2]. The FAT-CM is a linear device consisting of two conical theta-pinch formation sections and a confinement section in the middle. Initial plasmoids are formed via a field-reversal theta-pinch method using deuterium gas and translated to the confinement section along the magnetic pressure gradient of an external guide magnetic field [3]. The relative velocity of the initial plasmoids reaches 200 - 400 km/s during the translation.

In the experiment, several interesting phenomena are observed, such as self-organized FRC formation and shockwave generation [4]. A compact and component-based tomography camera (T-cam) has been developed as one of the non-invasive diagnostics of those events [5, 6].

The viewing angle of the T-cam was designed to cover the cross-section of FRCs with a typical diameter estimated via the excluded flux method [7]. However, experimental results show considerable radiation in the scrape-off layer during and after the collisional merging. Therefore, the reconstruction of internal structures was difficult during those phases. In this study, improved incident optical components have been developed and installed on the T-cam to capture the entire cross-section of the FRC plasma.

2. Arrangement of T-Cams on the FAT-CM

The collisional merging of plasmoids occurs in the middle of the confinement vacuum chamber with an inner diameter of ~0.8 m and total length of ~2 m. The collision of translated plasmoids occurs 20 - 30 μs after the formation, followed by a reformation of a FRC-like magnetic structure at ~70 μs [4]. The tomographic imaging system has been developed to observe these dynamic events on the order of microseconds. The system is arranged in the two cross sections of the confinement chamber ($z = \pm 0.3$ m), as shown in Fig 1. A set of two cameras and an anti-reflection plate are mounted on each cross-section.

The maximum viewing area is limited by the 6 in inner diameter of the ConFlat® viewing ports. In the previous setup, T-cams with a single cylindrical lens observed plasma from a flat quartz window [6]. Figure 2 shows the typical profiles observed using the previous design of T-

author's e-mail: asai.tomohiko@nihon-u.ac.jp

*) This article is based on the presentation at the 31st International Toki Conference on Plasma and Fusion Research (ITC31).

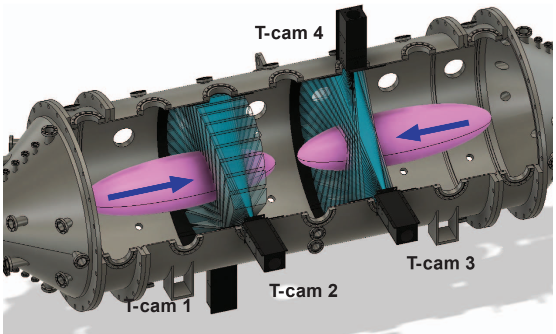

Fig. 1 Arrangement of T-cams on the confinement chamber.

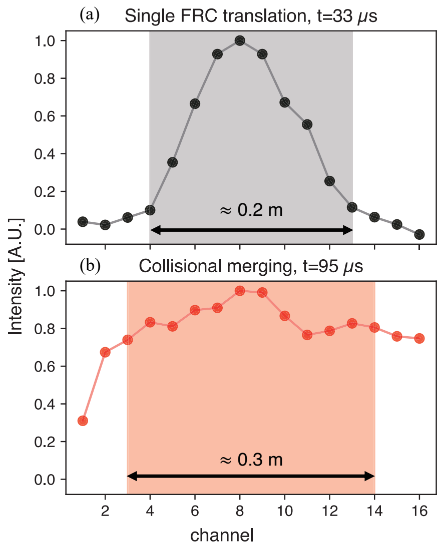

Fig. 2 Radiation profiles of (a) single FRC translation and (b) collisional merging cases captured using the previous T-cam design. The horizontal axis represents channels of multi-anode PMT mounted on T-cam. The gray and red shaded areas indicate FRC size. The edges correspond to the separatrix.

cams during the translation process and after merging.

In the case of single FRC translation (Fig. 2 (a)), the tail of the profile was clearly visible. The inflection point of the profile corresponds to the separatrix. On the other hand, considerable radiation was observed in the collisional merging case, as shown in Fig. 2 (b). This radiation was comparable to that in the core region outside of the separatrix (i.e., the scrape-off layer). Fig. 2 (b) captures the radiation profile in the post-collision equilibrium phase.

The viewing angle of each camera was designed to be approximately 60° to be able to observe the cross-section of FRCs with a typical plasma radius of 0.25 m at the collision. However, significant radiation outside the separatrix made it difficult to reconstruct the internal structure.

3. Improvement of the Field of View

The components of the newly designed T-cam consists of a 16-channel multi-anode photomultiplier tube (PMT),

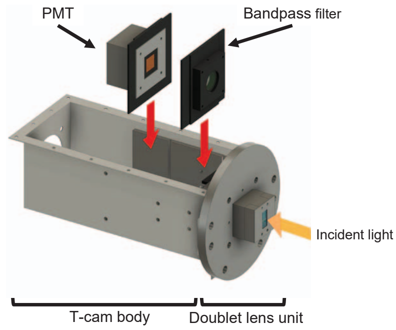

Fig. 3 3D schematic image of the newly-built T-cam.

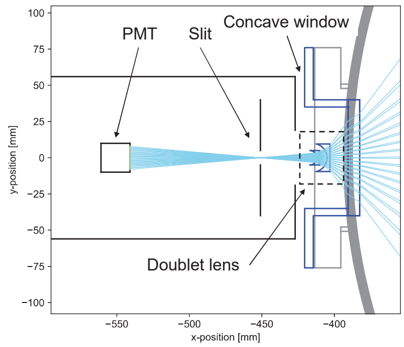

Fig. 4 Arrangement of the T-cam with newly-designed incident optical component.

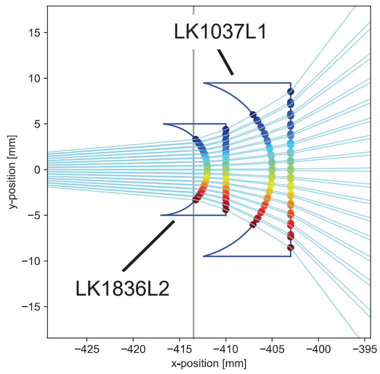

Fig. 5 Ray tracing diagram with lens configuration.

an optical bandpass filter, a slit, and a lens unit. These components are assembled within an electromagnetic/magnetic shield case made of ferritic stainless steel (SUS 430). Each component has a cartridge-type shape (Fig. 3). The component-based structure enables the modification of the wavelength band and field of view.

In the presented system, an optical bandpass filter with a center wavelength of 550 nm is installed to detect bremsstrahlung radiation in the visible light range. Instantaneous time response and a high sensitivity are required for the detectors. Therefore, a multi-anode PMT (R5900U-01-L16, Hamamatsu Photonics K.K.) is adopted as a detector [5,6]. The response time of the PMT is about 0.6 ns, which is fast enough to respond to and observe the sub-

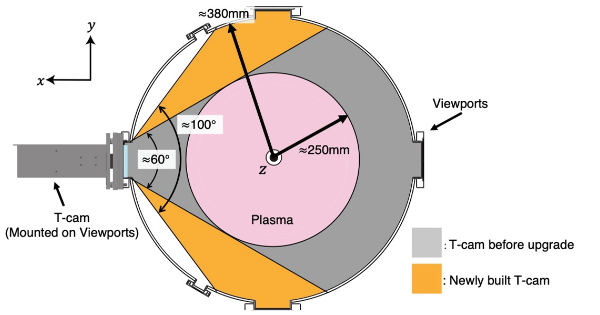

Fig. 6 Comparison of the field of view of newly built T-cam and the T-cam before upgrade. The pink circle indicates the typical cross-section of Merged-FRC.

microsecond behavior of the plasmoids.

Figure 4 illustrates the arrangement of the optical components including the newly-built incident optical unit with a doublet lens and a specially-designed concave window. The lens shape and arrangement were determined by ray tracing, as shown in Fig. 5. The concave window enables the installation of the doublet lens unit, which has been installed on the camera head. This unit includes two cylindrical lenses of different sizes (LK1836L2 and LK1037L1, Thorlabs, Inc), which approximately doubled the field of view. Figure 6 shows the field of view of the T-cams. The viewing angle is expanded from 60° - 100°. The observable range of the newly-developed T-cams covers most of the area inside the confinement chamber.

4. Performance Evaluation

The performance of the newly-built T-cam was evaluated via reconstruction with dummy data. The intensity of the bremsstrahlung radiation roughly depends on the electron density n_e and temperature T_e [8]. Assuming the uniform profile of T_e within the separatrix [9], the radiation coefficient of the bremsstrahlung radiation is proportional to n_e^2 [8, 10]. Thus, the dummy data was generated assuming the rigid rotor model (RRM), which is one of the equilibrium models for FRCs (Fig.7 (a)) [11]. Assuming charge neutrality, RRM determines the electron density profile inside the separatrix. The radial profile of electron density is written as:

$$n_e(r) = n_m \operatorname{sech}^2 K\left(\frac{r^2}{R^2} - 1\right), \quad (1)$$

$$K \equiv \tanh^{-1}\left(\frac{B_s}{B_e}\right), \quad (2)$$

where n_m, B_s, and B_e are the maximum densities at the magnetic axis, magnetic field on separatrix, and external magnetic field, respectively. The radius of the magnetic axis R is determined by the separatrix radius r_s as $R \equiv r_s/\sqrt{2}$ under the assumption of RRM. The dummy projection data was made by integrating $n_e(r)^2$ along the line of sight. Random noise of ±10% was superimposed onto the integrated data to simulate the actual measurement. The separatrix radius was set to 30 cm to evaluate the effect of widening the field of view.

Figure 7 shows a comparison of reconstructed images in the x-y plane: (a) the dummy radiation coefficient profile, (b) a reconstructed profile of the newly-built system, and (c) before improvement. The 1D graphs on the top and side of Figs. 7 (b) and (c) are radiation profiles on the x and y-axes. Each curve shows input projection data and the reconstruction. The reconstruction has been performed by the iterative calculation methods under the RRM [6]. Before the improvement, the reconstructed image is grossly distorted. On the other hand, the newly-developed system reproduced the dummy profile of the radiation coefficient.

5. Discussion and Summary

The T-cam with a newly designed doublet lens unit has provided a wide field of view, which is sufficient to observe the rapid expansion of FRCs during the collisional merging process. The performance evaluation was conducted with dummy data without the radial shift of the FRC axis. When a large deformation (toroidal mode number $n = 0$) and/or displacement ($n = 1$) occurs beyond the measurement area, the ordinary T-cam was unable to properly reconstruct the

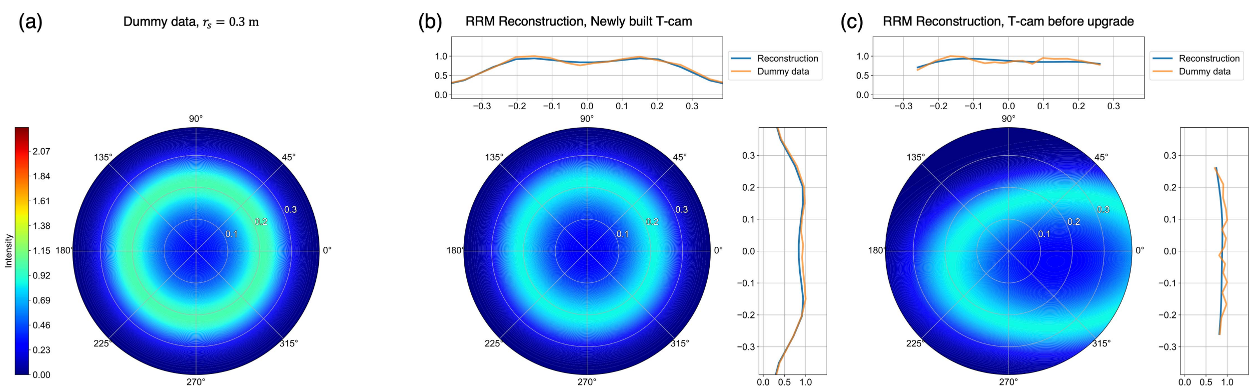

Fig. 7 Dummy profile (a) and comparison of a reconstructed image in the x-y plane with newly built T-cam (b) and before the improvement (c).

internal radiation profile. Additionally, the axis of the reconstructed image is shifted by the value that is comparable to the separatrix radius. If an FRC shifts by this amount, it hits a chamber wall. This result indicates that the T-cams before improvement cannot be applied as position monitors for an FRC. Therefore, the expanded field of view allows for a more accurate reconstruction of internal structures.

The newly-developed compact and component-based T-cam with fast response and expanded field of view enables observation of dynamic global motion during and after collision/merging, such as radial expansion ($n = 0$), wobble motion ($n = 1$), and growth of rotational instability ($n = 2$) occurring on the order of microseconds.

Acknowledgments

This work was partially supported by JSPS KAKENHI Grant No. JP20H00143 and the Grant for Project Research and the Grant for the Promotion of Leading Research, College of Science and Technology, Nihon University.

[1] L.C. Steinhauer, Phys. Plasmas **18**, 070501 (2011).
[2] T. Asai, T. Takahashi, J. Sekiguchi, D. Kobayashi, S. Okada *et al.*, Nucl. Fusion **59**, 056024 (2019).
[3] D. Kobayashi and T. Asai, Phys. Plasmas **28**, 022101 (2021).
[4] T. Asai, D. Kobayashi, T. Seki, Y. Tamura, T. Watanabe *et al.*, Nucl. Fusion **61**, 096032 (2021).
[5] H. Tomuro, T. Asai, K. Iguchi, T. Takahashi and Y. Hirano, Rev. Sci. Instrum. **81**, 10E525 (2010).
[6] T. Seki, T. Yamanaka, T. Asai, D. Kobayashi, T. Takahashi *et al.*, Rev. Sci. Instrum. **93**, 103520 (2022).
[7] M. Tuszewski and W.T. Armstrong, Rev. Sci. Instrum. **54**, 1611 (1983).
[8] T. Takahashi, H. Gota, T. Fujino, M. Okada, T. Asai *et al.*, Rev. Sci. Instrum. **75**, 5205 (2004).
[9] D.J. Rej and W.T. Armstrong, Nucl. Fusion **24**, 177 (1984).
[10] T. Asai, T. Takahashi, T. Kiguchi, Y. Matsuzawa and Y. Nogi, Phys. Plasmas **13**, 072508 (2006).
[11] W.T. Armstrong, R.K. Linford, J. Lipson, D.A. Platts and E.G. Sherwood, Phys. Fluids **24**, 2068 (1981).